


RESEARCH LETTER

Beta-amyloid interacts with and activates the long-form phosphodiesterase PDE4D5 in neuronal cells to reduce cAMP availability

Yuan Yan Sin¹, Ryan T. Cameron¹, Melissa Schepers^{2,3}, Ruth MacLeod¹, Tom A. Wright¹ , Dean Paes^{2,3}, Daniel van den Hove³, Emily Willems^{2,3}, Tim Vanmierlo^{2,3}, Jos Prickaerts³, Connor M. Blair¹ and George S. Baillie¹ 

¹ School of Cardiovascular and Metabolic Health, University of Glasgow, UK

² Department of Neuroscience, Biomedical Research Institute, Faculty of Medicine and Life Sciences, Hasselt University, Diepenbeek, Belgium

³ Department Psychiatry and Neuropsychology, School for Mental Health and Neuroscience, Maastricht University, The Netherlands

Correspondence

G. S. Baillie, School of Cardiovascular and Metabolic Health, College of Veterinary Medical and Life Science, University of Glasgow, Glasgow PA124EJ, UK
 Tel: +01413301662
 E-mail: george.baillie@glasgow.ac.uk

Yuan Yan Sin and Ryan T. Cameron can be considered joint first authors

(Received 16 January 2024, revised 15 April 2024, accepted 15 April 2024)

doi:10.1002/1873-3468.14902

Edited by Barry Halliwell

Inhibition of the cyclic-AMP degrading enzyme phosphodiesterase type 4 (PDE4) in the brains of animal models is protective in Alzheimer's disease (AD). We show for the first time that enzymes from the subfamily PDE4D not only colocalize with beta-amyloid (A β) plaques in a mouse model of AD but that A β directly associates with the catalytic machinery of the enzyme. Peptide mapping suggests that PDE4D is the preferential PDE4 subfamily for A β as it possesses a unique binding site. Intriguingly, exogenous addition of A β to cells overexpressing the PDE4D5 longform caused PDE4 activation and a decrease in cAMP. We suggest a novel mechanism where PDE4 long-forms can be activated by A β , resulting in the attenuation of cAMP signalling to promote loss of cognitive function in AD.

Keywords: Alzheimer's disease; beta-amyloid; cyclic AMP; PDE4

Cyclic-AMP (cAMP) signalling is a crucial pathway for memory formation/cognition and the down-regulation of this second messenger in the brain during Alzheimer's disease (AD) is thought to play a part in the cognitive deficits that are a characteristic of the disease [1,2]. cAMP-specific enzymes from the phosphodiesterase type 4 (PDE4) family have been identified as key players in shaping cerebral cAMP gradients that activate cAMP response element-binding protein (CREB) *via* PKA phosphorylation (reviewed in [3]). Several studies involving pharmacological inhibition [4–6], RNA

interference [7,8], dominant-negative PDE4 transfection [9], PDE4 knock-out mice [7] and CRISPR-Cas9 [10] have indicated that isoforms from the PDE4D subfamily are most influential as targets for therapeutic strategies. Recent evidence also supports the role of PDE4B in this regard [11]. Said strategies counteract the aberrant cAMP signalling that results in a down-regulation of CREB transcription factor activity and subsequent loss of synaptic plasticity. These observations have been supported by recent evidence from diseased human brains that show increased PDE4D expression when

Abbreviations

AD, Alzheimer's disease; APP/PS1, amyloid precursor protein/presenilin1; A β , β -amyloid; cAMP, cyclic AMP; CREB, cAMP response element-binding protein; FRET, fluorescence resonance energy transfer; GST, glutathione S-transferase; IBMX, 3-isobutyl-1-methylxanthine; mRNA, messenger RNA; PDE, phosphodiesterase; PDE4, phosphodiesterase type 4; PKA, protein kinase A; UCR, upstream conserved regions.

compared with controls [12]. Although mRNA transcripts [12] and western blotting [13] have been used to demonstrate elevated levels of PDE4D expression in AD models, there have been no attempts to look at the activation state of PDE4D enzymes during neurodegenerative disease. PDE4 enzymes, especially those designated as longforms, have an intrinsic activity that can be enhanced or inhibited by post-translational modification [14–16] or association with peptides [17] or lipids [18]. Here, we report that PDE4D enzymes colocalize with beta-amyloid (A β) plaques in brains of amyloid precursor protein/presenilin1 (APP/PS1) mice and that a direct association takes place between A β and the PDE4 enzyme. We provide peptide mapping evidence to show why PDE4D isoforms may have more relevance to AD than the other sub-families (PDE4A, B and C) and suggest that the low cAMP concentrations observed in AD brains may be a result of the activation of PDE4D longforms caused by direct A β association.

Materials and methods

Co-localization of PDE4D and A β

To investigate the potential formation of complexes between PDE4D and A β , mouse brain sections obtained from 7-month-old APP/PS1 Alzheimer's mice (MMRRC strain #034832-JAX) were subjected to dual staining for both markers. Initially, an antigen retrieval step was carried out by incubating the sections with 70% formic acid for 15 min, followed by thorough washing in tris-buffered saline (TBS). Subsequently, the sections were incubated overnight at 4 °C with a concentration of 2 $\mu\text{g}\cdot\text{mL}^{-1}$ rabbit anti-PDE4D (Abcam, Ab14613, Cambridge, UK) diluted in 0.3% TBS-T. Following the primary antibody incubation, sections were treated with a donkey anti-rabbit biotin secondary antibody (1/400 dilution in 0.3% TBS-T) (ThermoFisher, Loughborough, UK) for 1 h at room temperature. After completing TBS washing steps, sections were subjected to incubation with streptavidin-647 (1/500 in 0.3% TBS-T) (ThermoFisher) for an additional 1 h at room temperature to visualize PDE4D. Subsequent to the PDE4D visualization, the sections were further incubated overnight at 4 °C with a primary mouse anti-human A β , 17–24 antibody (clone 4G8) (BioLegend, San Diego, CA, USA, Ab800712) at a dilution of 1/500 in 0.3% TBST-T. The following day, sections were washed and subsequently incubated with a secondary anti-mouse AlexaFluor 488 antibody (1/250 in 0.3% TBS-T) (Invitrogen, Inchinnan, UK) for 1 h at room temperature. A Hoechst counterstain was performed to visualize cell nuclei.

To further validate PDE4D and A β colocalization within neurons, SHSY5Y cells (sourced from ATCC within last 3 years) (RRID:CVCL_0019) were plated at 50 000 cells

on glass coverslips and cultured in DMEM/F-12 (Gibco, Grand Island, NY, USA) supplemented with 10% foetal bovine serum, 1% L-glutamine, 1% nonessential amino acids and 1% penicillin/streptomycin mixture until ~ 80% confluency. Cells were routinely checked for mycoplasma. Cells were then treated with 5 μM FAM-A β (Anaspec, Kidderminster, UK) for 1 or 24 h and fixed in 4% paraformaldehyde. Blocking with 1% BSA and 0.1% Tween80 was performed, followed by overnight incubation with a primary PDE4D antibody (Abcam, ab14613) and a 1 h incubation with an Alexa fluor 555 secondary antibody (Invitrogen, A31572). Counterstaining was done using DAPI dye and coverslips were mounted using fluoromount (Invitrogen). Samples were imaged using the Zeiss LSM900 confocal microscope using a 63 \times oil objective. Z-stacks were obtained and processed in ZEN 3.4 LITE (Zeiss, Cambridge, UK) and FIJI IMAGE J software (Fuji, Madison, WI, USA). Colocalization of PDE4D and FAM was determined using the IMAGE J colocalization threshold plugin.

Fluorescence polarization

Fluorescence polarization measurements were performed on a Mithras LB 940 plate reader (Berthold Technologies, Bad Wildbad, Germany) with the excitation and emission wavelengths 485 and 535 nm respectively. All FAM-A β peptides (1–40) were synthesized by AnaSpec and dissolved in DMSO to a stock concentration of 10 mM. The assay was formatted using 10 μL reaction volume per well in non-binding, black 384-well plates (Cat no. # 262260) and Thermo Fisher Scientific Assay buffer (PBS, 1 mM DTT and 0.25% Tween-20) was used to dilute all ingredients. All polarization values are expressed in millipolarization units (mP). A fixed concentration of 10 μM FAM-A β (1–40) was used with increasing amounts of GST and GST-PDE4D5. Reactions were incubated for 30 min at room temperature in the dark. In order to examine the existence of non-specific binding, GST protein was used as a negative control. All the experiments were independently repeated at least thrice.

Peptide array

The PDE4 isoform sequence peptide arrays were synthesized as sequential 25mers shifted by 5 amino acids *via* SPOT synthesis [19] on continuous cellulose membranes using Fmoc-chemistry with a MultiPep 2 instrument (CEM Corporation, Matthews, NC, USA). For the alanine scanning arrays, versions of arrays were synthesized to incorporate alanine residues in place of the endogenous amino acid. In the event of alanine being the original residue, an aspartic acid or glycine was incorporated. The membranes were blocked with 5% milk/TBST (w/v) for 1 h. The PDE4 arrays were then overlaid with either A β _{1–42} or A β _{scr} (Anaspec) overnight at 4 °C. The arrays were then analysed

utilizing a far-western immunoblotting approach. Analogous methods were used to probe overlapping A β_{1-42} arrays with GST-fusion PDE4D5 protein in order to determine which domains within A β_{1-42} are responsible for binding PDE4s. Specifically, A β_{1-49} arrays were overlain with PDE4D5-GST and a mouse monoclonal GST-HRP (Sigma, A7340, Lee on the Solent, UK) was used at 1 : 5000 for 2 h at room temperature to detect binding.

Co-immunoprecipitation

SHSY-5Y cells cultured in six-well plates were treated with either 10 μ M A β_{1-42} or A β_{scr} for 24 h. The neurotoxin 10 μ M A β_{1-42} derivatives were created as previously described [20]. Cellular lysates were prepared in lysis buffer [25 mM HEPES, 2.5 mM EDTA, 50 mM NaCl, 50 mM NaF, 30 mM sodium pyrophosphate, 10% (v/v) glycerol and 1% (v/v) Triton X-100, pH 7.5, containing Complete™ EDTA-free protease inhibitor cocktail tablets (Roche, Welwyn Garden City, UK)] after the treatment. Protein concentration of lysates was determined using the Bradford assay and all samples were equalized for protein concentration (400 μ g protein per IP reaction). Goat anti-Pan-PDE4D antibody (in-house) was used to immunoprecipitate endogenous A β . The resulting immunocomplexes were captured using 25 μ L of Protein G magnetic beads per sample (Pierce #88847, Huddersfield, UK) at 4 °C overnight with mixing. Normal goat IgG (Bio-Techne Ltd, #AB-108-C, Minneapolis, MN, USA) was used as a mock IP control. The beads were washed three times using lysis buffer. Bound proteins were then eluted in SDS/PAGE sample buffer and subjected to SDS/PAGE for immunoblotting using mouse anti-A β antibody (Sigma #A8354, 1 : 5000), followed by goat anti-Pan-PDE4D antibody (in-house, 1 : 5000) to confirm protein input. Immunoreactive proteins were detected by IRDye 680RD donkey anti-mouse IgG (Li-COR, #926-68072, Lincoln, NE, USA) and Alexa Fluor 790 donkey anti-goat IgG (Abcam, #ab175784) respectively. Images were acquired using Li-Cor Odyssey CLx Imaging System and signals were detected at 700 and 800 nm channels.

Proximity ligation assay

SH-SY5Y cells cultured in eight-well chamber slides (Falcon #354118; Fisher Scientific, Waltham, MA, USA) were treated with either 10 μ M A β_{1-42} or A β_{scr} (Anaspec) for 24 h. The cells were fixed with 4% (v/v) paraformaldehyde in PBS for 15 min at room temperature. Cells were counterstained with cell surface marker wheat germ agglutinin (WGA) conjugated to AlexaFluor 488 (Invitrogen #W11261) for 5 min, followed by permeabilization using 0.1% Triton X-100 (Sigma-Aldrich) in PBS for 10 min at room temperature. *In situ* detection of the exogenous A β and PDE4D protein–protein interaction was carried out

utilizing Duolink® proximity ligation assay [21] as per manufacturer's instructions (Duolink®, Merck, Irvine, UK). Equal concentrations (1 : 4000) of immunocytochemistry-validated PDE4D (goat) and A β (mouse) primary antibodies were used in combination with respective Duolink® PLA anti-goat (PLUS) and anti-mouse (MINUS) probes. Slides were finally mounted under coverslips with Prolong Gold Antifade reagent with DAPI (Invitrogen, P36935) and visualized. Images were acquired using an upright Zeiss LSM 880 confocal laser scanning microscope under a 63 \times oil immersion objective (excitation 594 nm and emission 624 nm). In order to detect all PLA signals, a series of Z-stack images were collected and analysed by IMAGEJ software.

PDE4 activity assays

An expression pCDNA3 plasmid encoding human PDE4D5-VSV was used before by us [22], which was prepared using the Maxi-prep system (Qiagen, Dusseldorf, Germany). For transient transfections, SH-SY5Y cells were transfected using PolyFect® transfection reagent (Qiagen) in accordance with manufacturer's instructions. Cells (~90–100% confluent) were transfected for 48 h with cDNA-encoding PDE4D5 and treated for 6 h with A β_{1-42} or A β_{scr} . Cells were then washed with PBS and harvested by using a cell scraper in KHEM buffer (50 mM KCl, 50 mM HEPES; pH 7.2, 10 mM EGTA, 1.92 mM MgCl₂ and 1 mM dithiothreitol (DTT)) supplemented with protease inhibitor Mini-Complete (Roche). Samples were then frozen on solid CO₂, thawed and then manually homogenized, followed by passage through a 26-gauge needle several times to ensure complete cell lysis. Cells were centrifuged at 20 784 *g* for 10 min to remove any unbroken cells, and the resulting supernatant was frozen in solid CO₂ and stored at –80 °C until required. For experimentation, the protein concentration of whole-cell lysate from transfected and mock-transfected (vector only) cells was equalized (typically to 1 μ g· μ L⁻¹). Protein concentration was determined through Bradford assay using bovine serum albumin as standard. PDE activity was determined using a two-step radioassay procedure as described previously [23]. Activities were related to a non-treated sample (100% control) over an increasing dose of the A β_{1-42} or A β_{scr} . In all cases, the transfected PDE accounted for over 97% of the total PDE activity when compared with the untransfected control lysates.

cAMP FRET reporter assay

Assays were conducted as previously described [24]. HEK293 cells were seeded onto sterile glass coverslips and incubated for 24 h. The cells were transiently transfected with a cAMP monitoring FRET sensor based on the

structure of EPAC1 (EPAC1-cAMPs) [25] using Lipofectamine LTX (Invitrogen). FRET imaging was performed 24 h following transfection and 60 min following pre-incubation with DMSO, A β _{1–42} or A β _{scr}. For imaging, the cells were buffered in a solution of 125 mM NaCl, 5 mM KCl, 20 mM HEPES, 1 mM Na₃PO₄, 1 mM MgSO₄, 1 mM CaCl₂ and 5.5 mM glucose, pH 7.4, and stimulated with 1 μ M forskolin followed by a cAMP saturating concentration of 25 μ M forskolin and the non-specific PDE inhibitor IBMX (100 μ M). Analysis was undertaken using an Olympus IX71 inverted microscope with a 60 \times oil immersion objective (Zeiss, Cambridge, UK) and an optical beam splitter (Photometrics, Tucson, AZ, USA). METAFLUOR software (Molecular Devices, San Jose, CA, USA) allowed image acquisition and real-time monitoring. FRET changes were measured by excitation at 440 nm and obtaining a ratio of the intensity of emissions at 480 and 545 nm. Data are expressed as the % FRET change normalized to the baseline FRET ratio at $t = 0$.

Mice

The postmortem brain tissue used was derived from animals used in a previous study [10]. All animal experiments were approved by the local ethical committee of Hasselt University for animal experiments (matrix ID 201838) and met governmental and institutional guidelines. Female transgenic Alzheimer mice (APP^{swe}/PS1^{dE9} on C57bl/6 background) were generated in an in-house breeding (matrix ID 201759). Mice were genotyped by PCR analysis of ear biopsies. At the age of 7 months, animals were housed individually in standard cages. They were kept under a reversed 12/12 h light/dark cycle and food and water were provided *ad libitum*. At 8 months of age, animals were perfused with PBS-heparin, and brain sections were made by cryostat.

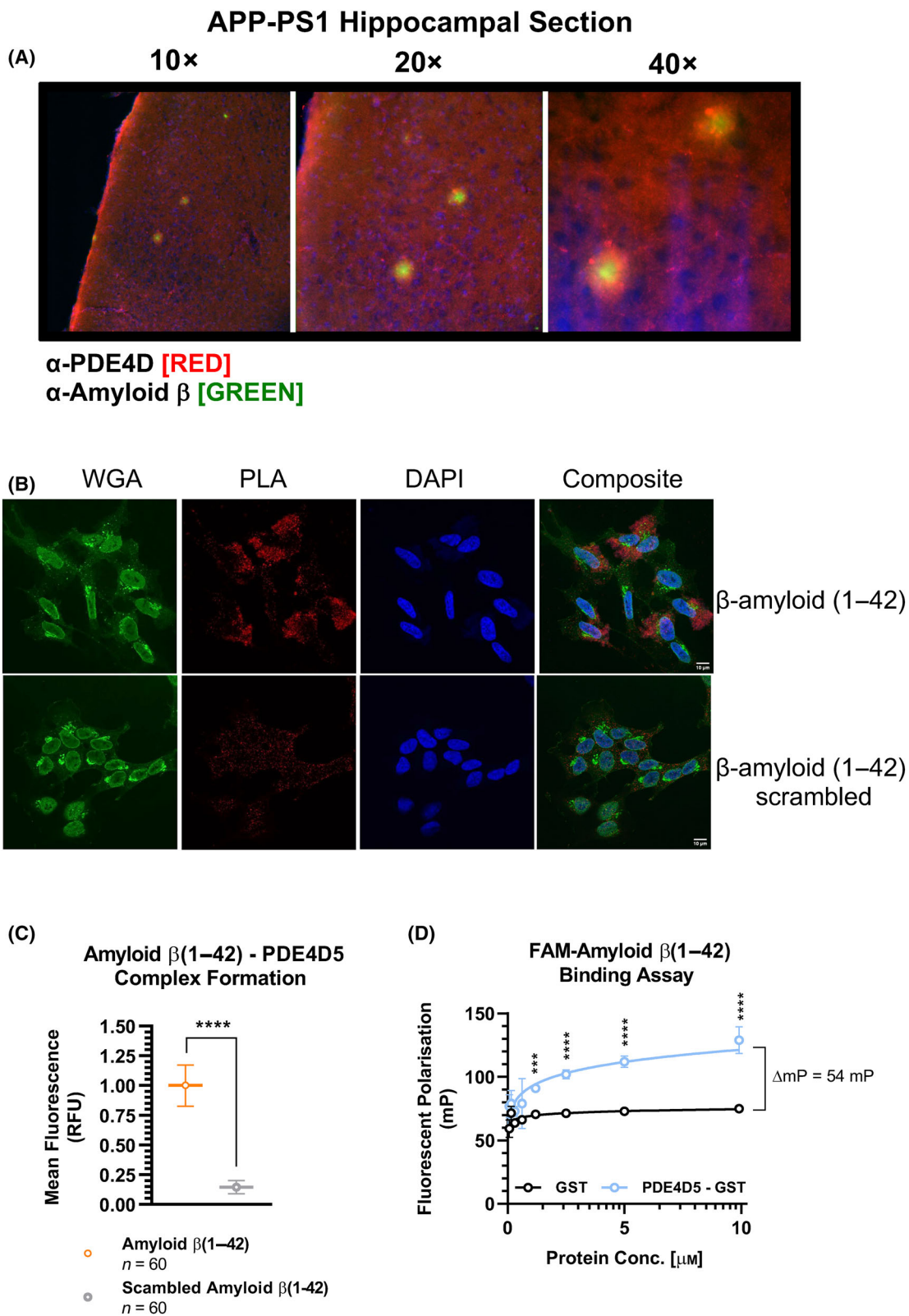
Results

As previous work has indicated that increases in expression of PDE4B and D enzymes are associated with cognitive impairment in AD [12,13,26,27], we decided to stain hippocampal slices taken from APP/PS1 mice with antibodies raised against PDE4D

and an antibody that detects A β . Magnification at 10 \times and 20 \times allowed clear observation of co-localization between the phosphodiesterase and A β in plaques that were surrounded by cells expressing PDE4D at a higher level than those positioned more remotely from plaques (Fig. 1A). This was not an artefact of non-specific staining, as plaques formed on coverslips by FAM-A β _{1–42} were not recognized by the PDE4D antibody (Fig. S1). We also recreated this experiment *in vitro* using exogenous addition of A β to cultured SH-SY5Y cells (Fig. S2) and again we detected an intracellular colocalization of PDE4D and A β . Co-localization was seen both at 1 h when FAM-A β was intracellular but diffuse and at 24 h when intracellular aggregates had formed (Fig. S2). To further support this notion, we utilized proximity ligation (PLA), a technique which we have used before to visualize co-segregation of PDE4 and binding partners [28]. PDE4D and A β _{1–42} could be detected in close proximity in the cytoplasm, but not in nucleus of SH-SY5Y cells (Fig. 1B) and there was significantly more PLA signal when cells were treated with A β _{1–42} compared with A β _{1–42} scrambled (Fig. 1C). As this is the first indication that PDE4D and A β exist in close proximity inside brain cells, we used a biophysical assay to assess the likelihood that the PDE4 and A β could associate directly. Fluorescence polarization experiments using fluorescently labelled 1–42 A β peptide indicated a dose-dependent association with GST-tagged PDE4D5 but not with GST alone (Fig. 1D). Additionally, using a technique previously used to investigate the interaction of A β with VDAC1 [29] we were able to co-immunoprecipitate A β with PDE4D from SH-SY5Y cells pre-treated with the peptide (Fig. S3). The co-immunoprecipitating A β bands were at molecular weights observed in the prior study [29].

The direct interaction between PDE4 proteins and A β detected in Fig. 1 allowed us to map the binding sites by peptide array, a technique that we have used on multiple occasions to discover PDE-binding partner docking domains [24,30,31]. Immobilized libraries of PDE4 sequences corresponding to PDE4A4 (Fig. 2B),

Fig. 1. PDE4D and A β form complexes. (A) Naive APP/PS1 mouse brain sections from mice aged 7 months were stained for PDE4D (647, red) and A β (488, green) to determine colocalization. Pictures taken at 10 \times , 20 \times and 40 \times magnifications show that PDE4D and A β co-localize with each other in plaques. Sections were counterstained with Hoechst to visualize cell nuclei. (B) Proximity ligation assays were done on SH-SY5Y cells following treatment with 10 μ M A β _{1–42} or A β _{scr} for 24 h. Antibodies against PDE4D pan and A β were used in PLA assay. Cells were counterstained with AlexaFluor488-conjugated wheat germ agglutinin to improve cell segmentation. Scale bar = 10 μ m. (C) Quantification of mean fluorescence PLA signal per cell ($n = 3$, 60 cells per condition). Evaluated with student's *T*-test, **** = $P < 0.0001$. Error bars represent SEM. (D) Fluorescence polarization determination of GST or GST-PDE4D5 binding to increasing concentrations of FAM-A β (1–40). Results $n = 3$. Evaluated with student's *T*-test, *** = $P < 0.001$ **** = $P < 0.0001$.



PDE4B1 (Fig. 2C), PDE4D5 (Fig. 2D) and PDE4D7 (Fig. 2E) were constructed as 25mers sequentially shifted by 5 amino acids. Arrays encompassing the whole sequence of each PDE4 were overlain with 1–42 A β peptide or a scrambled control version. Arrays were then blotted for A β , with dark spots signifying a direct interaction between the immobilized PDE4 sequence 25mer and A β . Figure 2A depicts the modular structure of PDE4 enzymes, with the conserved catalytic region following on from the two regulatory regions (UCR1 and 2) and the N-terminal targeting domain that is unique to each isoform. Interestingly, A β bound to all four isoforms of PDE4 in a region close to the start of the catalytic unit. The A β binding region on PDE4s has three putative binding motifs, one of which is unique to PDE4D isoforms (Site 3 outlined in Fig. 2A). Firstly, there is a double-lysine ('KK', Site 1) motif that appears in all PDE4s (except PDE4C) and starts only 8 amino acids from the start of the catalytic unit (Fig. 2A, lower panel). Point alanine substitution of either of the lysines dramatically reduced A β binding to PDE4B sequences, whereas a double-alanine substitution was required to decrease binding to PDE4D and ablate PDE4B and PDE4A association (Fig. 3A). Secondly, the arginine–phenylalanine ('RF', Site 2) motif appears in all PDE4 enzymes and alanine substitution of the 'R' ablates A β binding to PDE4B and dramatically reduces binding to PDE4A and D (Fig. 3A). Substitution of the 'F' with alanine slightly reduced PDE4A and D binding and dramatically reduced PDE4B association. Double substitution of the 'RF' motif to alanine ablated PDE4B binding and attenuated that of PDE4A and D. Quadruple substitution of all four residues in both motifs resulted in a complete loss of A β association with the PDE4 sequences (Fig. 3A). Site 3 is unique to PDE4D isoforms and appears in a rare region of the catalytic site that is less well conserved than the other parts (Fig. 3A, lower panel). Alanine scanning analysis shows that each of the residues depicted in bold at the top of Fig. 3B is essential for A β binding to PDE4D.

The A β -binding sequence was superimposed onto an existing crystal structure of a PDE4D catalytic domain dimer (PDB: 7XAB) [32]. The binding site is external to the dimerization interface and is composed primarily of α -helical secondary structure (Fig. 3C).

As we have discovered A β binding sites on PDE4 sub-family members, we investigated potential complementary PDE4 binding sites on the A β peptide sequence using peptide array. Using APP transmembrane domain (D672 – L720) which corresponds (following sequential proteolytical cleavage) to the A β peptide sequence, we constructed arrays consisting of 20mers, sequentially shifted by 2 amino acids and overlaid these peptide spots with purified PDE4D5-GST or GST alone as a negative control (Fig. 4). In doing so, we identified one 20mer sequence (G696-V715) that bound strongly to PDE4D5-GST but not GST alone (Fig. 4A). Point alanine (Fig. 4B) and truncation (Fig. 4C,D) analysis of the A β 20mer identified that K699 was essential for the association of PDE4D5 and A β . The A β mutants K699D and N698E also ablated binding (Fig. 4B, third and second last spots), suggesting that a salt bridge may form between A β and negatively charged residues on PDE4D5. Visualizing the PDE4 binding sequence on an existing 3D structure (solution NMR) of the APP Q686–K726 dimer (PDB: 2LOH) [33] reveals PDE4D5 binding to the dimerization interface, suggesting PDE4D5 binding may influence the dimerization/oligomerization of A β (Fig. 4E).

In light of the fact that FP and peptide array have indicated that A β may form a complex with PDE4D proteins in the catalytic region, and in cognizance of recent reports that there is an insignificant change in PDE4D expression in the hippocampus of the APP/PS1 mice compared with WT but a highly significant threefold change in PDE4 activity [10], we next wanted to check whether PDE4 activity is altered following A β binding. Addition of increasing concentrations of A β _{1–42} and A β _{1–42} scrambled to cells overexpressing PDE4D5 isoforms followed by

Fig. 2. Peptide mapping of A β binding domains on PDE4. (A) Upper panel depicts the modular structure of PDE4 long-form enzymes showing the N-terminal unique region, upstream conserved region 1 (UCR1) and upstream conserved region 2 (UCR2), core catalytic region and sub-family-specific C-terminal region. Lower panel depicts the amino acid sequences of three A β binding sites at the start of the catalytic unit for each of the different sub-families (PDE4A, PDE4B, PDE4C and PDE4D). (B) Sequential 5-amino shift of PDE4A4 sequence with site 1 and site 2 depicted in bold/underlined. Control is overlain with scrambled A β . (C) Sequential 5-amino shift of PDE4B1 sequence with site 1 and site 2 depicted in bold/underlined. Control is overlain with scrambled A β . (D) Sequential 5-amino shift of PDE4D5 sequence with site 1, site 2 and site 3 depicted in bold/underlined. Control is overlain with scrambled A β . (E) Sequential 5-amino shift of PDE4D7 sequence with site 1, site 2 and site 3 depicted in bold/underlined. Control is overlain with scrambled A β . All peptide array experiments were repeated $n = 2$.

assessment of PDE4 activity in cell lysates showed that A β could activate PDE4D5 whereas scrambled A β could not (Fig. 5A). Using a transfected cytosolic FRET-based cAMP-reporter (Fig. 5B), we observed a reduction in cellular levels of cAMP following treatment with a sub-optimal concentration of the adenylyl cyclase activator Forskolin (1 μ M), where cells were pre-treated with A β_{1-42} for 2 h (Fig. 5D). This was not observed with A β_{1-42} scrambled control peptide (Fig. 5E) or DMSO control (Fig. 5C). Statistics is shown in Fig. 5F. Although small but significant changes in cAMP were detected, these data once again suggest that PDE4 activity was increased when exposed to A β . There was no difference between treatments when the probes were saturated following treatment with IBMX and forskolin (Fig. 5F) with the maximal FRET change being approximately 20% (Fig. 5F).

Discussion

Many review articles [34,35] have catalogued the variety of benefits afforded by PDE4 and PDE4D selective inhibitors [6] in models of AD. Indeed, other ways of attenuating PDE4D activity (e.g. siRNA [36], dominant negatives [9] and genetic silencing [7]) have also provided rescue from maladaptations conferred by a down-regulation of cAMP signalling associated with loss of synaptic plasticity. Recent reports of increased PDE4D expression in human AD brains [12] and animal AD model brains [37] are also consistent with the studies describing decreased phospho-CREB in AD models and may represent one reason why PDE4 inhibition is so effective in this disease context. Robust evidence supporting a similar role for PDE4B has also recently been published [11,26,27]. One point that has not been addressed to date is the possible activation of PDE4 longforms during AD progression.

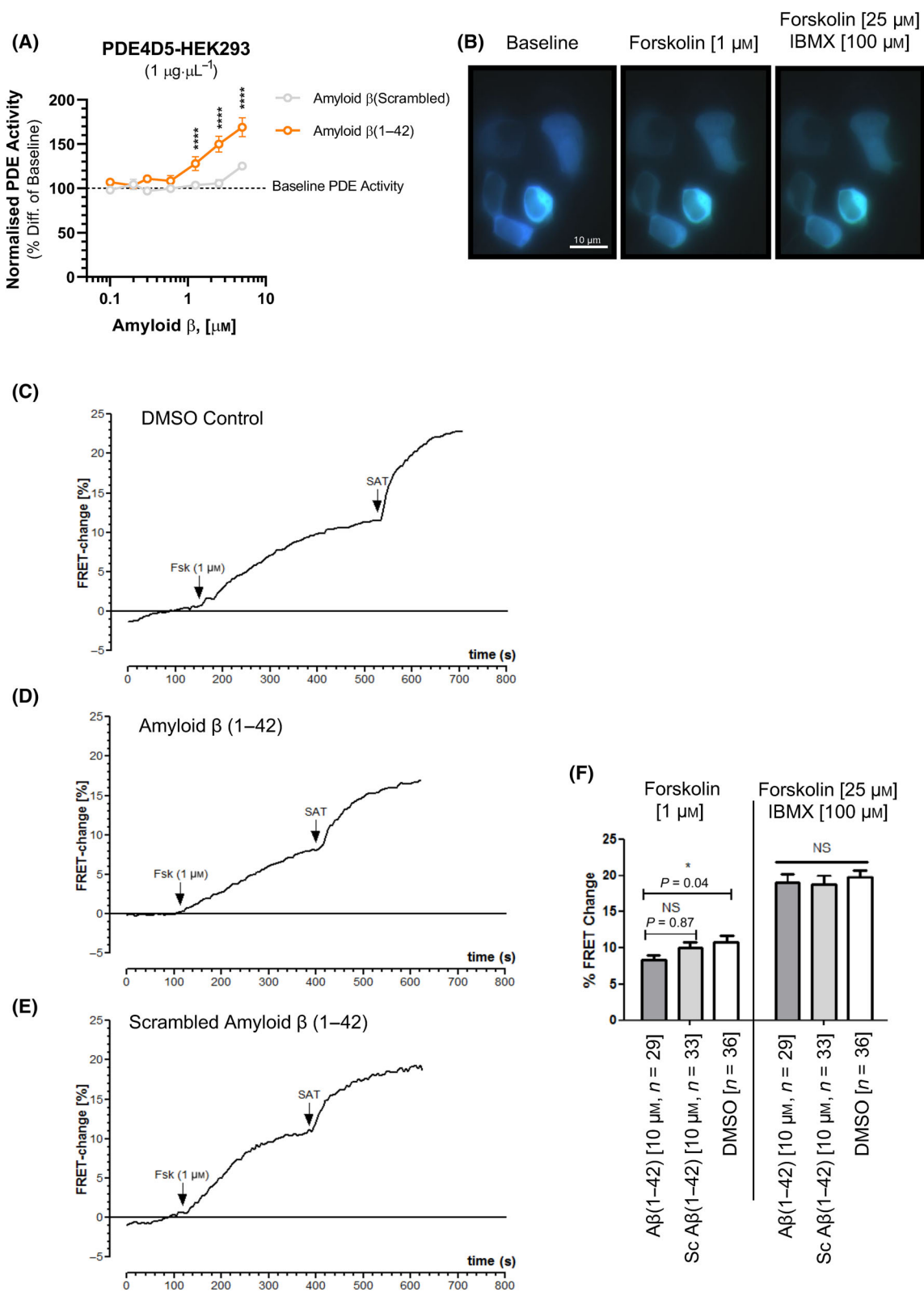
Previous work using human protein microarrays had shown that A β and PDE4 can physically interact [38] and in line with our data, only the PDE4D subfamily showed a robust interaction. We provide evidence that

A β binds directly to PDE4D in a region at the start of the catalytic core and that this event activates the long-form enzyme PDE4D5 (Fig. 5A). Such an action could facilitate a reduction in cAMP (Fig. 5F) that results in a loss of phospho-CREB. It is possible that the A β peptide in some way relieves the UCR2 ‘transcapping’ of active sites only observed in PDE4 dimers [39]. A similar mode of activation has recently been described for allosteric PDE4 activator compounds that phenocopy the actions of PKA phosphorylation of UCR1 [40]. Similar activations of PDE4 longforms can also be triggered by antibodies against UCR2, peptide fragments of the regulatory regions and phosphatidic acid (summarized in [41,42]). All of these are thought to bind to the PDE4 enzyme to confer stabilization of PDE4 dimers in conformations that relieve the auto-inhibition by UCR2 transcapping. Hence, it is possible that the A β -activation mechanism of PDE4 longforms is similar, although structural work and experiments with PDE4 phospho-mimic mutants would be required to confirm this.

In converse experiments, PDE4D5 was shown to bind to an A β -site containing K699 (Fig. 4). This region is known to be crucial for self-assembly of toxic oligomers and fibrils [43,44] suggesting that PDE4D5 may prevent or reverse A β oligomerization. We have already shown that a PDE4D-binding partner, HSP20, can bind to the oligomerization domain of A β when HSP20 has been phosphorylated by PKA [20]. This action is facilitated by PDE4 inhibition which promotes HSP20 serine 16 phosphorylation by PKA [24] and promotes HSP20-A β interaction in order to prevent A β oligomerization [20]. It is possible that HSP20 is maintained in its inactive (non-phospho) form in a three-way PDE4-HSP20-A β complex where the activating action of A β on PDE4 keeps local cAMP concentrations low.

Finally, we show that PDE4D intimately localizes with A β in hippocampal cells from APP/PS1 mice. This is to our knowledge the first report of such a relationship where PDE4D expression seems to be enhanced around the areas where plaques have

Fig. 5. PDE4 longforms are activated by A β . (A) SH-SY5Y cells transfected with PDE4D5 were treated for 6 h with indicated concentrations of A β_{1-42} or A β_{scr} . before lysates were harvested and evaluated for rolipram-inhibited PDE4 activity. Activity is normalized to lysate from non-treated transfected cells. $n = 3$ Error bars represent SEM. (B) HEK293 cells were transfected with the cAMP reporter EPAC1-cAMPs and treated as indicated. The images show representative images that allow visualization of reporter. Scale bar = 10 μ m (C) Transfected HEK293 cells were pre-treated with DMSO and the reaction to 1 μ M forskolin was monitored. (D) Transfected HEK293 cells were pre-treated with 10 μ M A β_{1-42} and the reaction to 1 μ M forskolin was monitored. $n = 3$, 15 cells per treatment. (E) Transfected HEK293 cells were pre-treated with 10 μ M A β_{scr} and the reaction to 1 μ M forskolin was monitored. $n = 3$, 15 cells per treatment. (F) Quantification of relative FRET changes produced in response to 1 μ M Forskolin (left) or 25 μ M Forskolin plus 100 μ M IBMX. $n = 3$, 15 cells per treatment. Students t -test $*P < 0.05$. Error bars represent SEM.



formed. This could be related to possible anti-aggregation effect of PDE4D5 that sequesters monomeric A β . Additionally, as we have also shown the intracellular colocalization of PDE4D and exogenously applied A β , albeit in a cultured cell line, we speculate that cells located around plaques may have increased cytoplasmic A β and therefore enhanced PDE4 activity. We appreciate that this mechanism is yet to be proven in human brains, however, as it is known that PDE4D selective inhibitors reverse learning and memory deficits in this mouse model *via* PKA and phospho-CREB (summarized in [3]), the robustness of that effect may be down to the fact that concentrated areas of A β -activated PDE4D enzymes are depressing local cAMP concentrations.

In summation, our data suggest a new molecular mechanism by which A β can down-regulate cAMP in order to promote cognitive deficits associated with AD.

Acknowledgements

The authors would like to thank Professor Manuela Zaccolo for supplying the cAMP reporter constructs (EPAC1-cAMPs). This work was supported by a doctoral training studentship from the Biotechnology and Biological Sciences Research Council [grant number BB/F016735/1].

Author contributions

GSB, YYS, JP, TV, CMB and RTC devised and designed project; YYS, RTC, MS, RM, TAW, DP, DH and EW acquired and interpreted the data; GSB, YYS and CMB wrote the first draft of the paper; and GSB, JP and TV edited the final version.

Peer review

The peer review history for this article is available at <https://www.webofscience.com/api/gateway/wos/peer-review/10.1002/1873-3468.14902>.

Data accessibility

All data sets that were used to construct this manuscript are available on request.

References

- Ricciarelli R and Fedele E (2018) cAMP, cGMP and amyloid beta: three ideal Partners for Memory Formation. *Trends Neurosci* **41**, 255–266.
- Sharma VK, Singh TG and Singh S (2020) Cyclic nucleotides signaling and phosphodiesterase inhibition: defying Alzheimer's disease. *Curr Drug Targets* **21**, 1371–1384.
- Tibbo AJ, Tejada GS and Baillie GS (2019) Understanding PDE4's function in Alzheimer's disease; a target for novel therapeutic approaches. *Biochem Soc Trans* **47**, 1557–1565.
- Cui SY, Yang MX, Zhang YH, Zheng V, Zhang HT, Gurney ME, Xu Y and O'Donnell JM (2019) Protection from amyloid beta peptide-induced memory, biochemical, and morphological deficits by a phosphodiesterase-4D allosteric inhibitor. *J Pharmacol Exp Ther* **371**, 250–259.
- Sierksma AS, van den Hove DLA, Pfau F, Philippens M, Bruno O, Fedele E, Ricciarelli R, Steinbusch HWM, Vanmierlo T and Prickaerts J (2014) Improvement of spatial memory function in APPswe/PS1dE9 mice after chronic inhibition of phosphodiesterase type 4D. *Neuropharmacology* **77**, 120–130.
- Ricciarelli R, Brullo C, Prickaerts J, Arancio O, Villa C, Rebosio C, Calcagno E, Balbi M, van Hagen BTJ, Argyrousi EK *et al.* (2017) Memory-enhancing effects of GEBR-32a, a new PDE4D inhibitor holding promise for the treatment of Alzheimer's disease. *Sci Rep* **7**, 46320.
- Li YF, Cheng YF, Huang Y, Conti M, Wilson SP, O'Donnell JM and Zhang HT (2011) Phosphodiesterase-4D knock-out and RNA interference-mediated knock-down enhance memory and increase hippocampal neurogenesis via increased cAMP signaling. *J Neurosci* **31**, 172–183.
- Shi Y, Lv J, Chen L, Luo G, Tao M, Pan J, Hu X, Sheng J, Zhang S, Zhou M *et al.* (2021) Phosphodiesterase-4D knockdown in the prefrontal cortex alleviates memory deficits and synaptic failure in mouse model of Alzheimer's disease. *Front Aging Neurosci* **13**, 722580.
- Bolger GB, Smoot LHM and van Groen T (2020) Dominant-negative attenuation of cAMP-selective phosphodiesterase PDE4D action affects learning and behavior. *Int J Mol Sci* **21**, 5704.
- Paes D, Schepers M, Willems E, Rombaut B, Tiane A, Solomina Y, Tibbo A, Blair C, Kyurkchieva E, Baillie GS *et al.* (2023) Ablation of specific long PDE4D isoforms increases neurite elongation and conveys protection against amyloid-beta pathology. *Cell Mol Life Sci* **80**, 178.
- Armstrong P, Gungör H, Anongjanya P, Tweedy C, Parkin E, Johnston J, Carr IM, Dawson N and Clapcote SJ (2024) Protective effect of PDE4B subtype-specific inhibition in an app knock-in mouse model for Alzheimer's disease. *Neuropsychopharmacology* doi: 10.1038/s41386-024-01852-z
- Paes D, Lardenoije R, Carollo RM, Roubroeks JAY, Schepers M, Coleman P, Mastroeni D, Delvaux E,

- Pishva E, Lunnon K *et al.* (2021) Increased isoform-specific phosphodiesterase 4D expression is associated with pathology and cognitive impairment in Alzheimer's disease. *Neurobiol Aging* **97**, 56–64.
- 13 Wang G, Chen L, Pan X, Chen J, Wang L, Wang W, Cheng R, Wu F, Feng X, Yu Y *et al.* (2016) The effect of resveratrol on beta amyloid-induced memory impairment involves inhibition of phosphodiesterase-4 related signaling. *Oncotarget* **7**, 17380–17392.
 - 14 MacKenzie SJ, Baillie GS, McPhee I, MacKenzie C, Seamons R, McSorley T, Millen J, Beard MB, van Heeke G and Houslay MD (2002) Long PDE4 cAMP specific phosphodiesterases are activated by protein kinase A-mediated phosphorylation of a single serine residue in upstream conserved region 1 (UCR1). *Br J Pharmacol* **136**, 421–433.
 - 15 Li X, Vadrevu S, Dunlop A, Day J, Advant N, Troeger J, Klussmann E, Jaffrey E, Hay RT, Adams DR *et al.* (2010) Selective SUMO modification of cAMP-specific phosphodiesterase-4D5 (PDE4D5) regulates the functional consequences of phosphorylation by PKA and ERK. *Biochem J* **428**, 55–65.
 - 16 Baillie GS, MacKenzie SJ, McPhee I and Houslay MD (2000) Sub-family selective actions in the ability of Erk2 MAP kinase to phosphorylate and regulate the activity of PDE4 cyclic AMP-specific phosphodiesterases. *Br J Pharmacol* **131**, 811–819.
 - 17 Wang L, Burmeister BT, Johnson KR, Baillie GS, Karginov AV, Skidgel RA, O'Bryan JP and Carnegie GK (2015) UCR1C is a novel activator of phosphodiesterase 4 (PDE4) long isoforms and attenuates cardiomyocyte hypertrophy. *Cell Signal* **27**, 908–922.
 - 18 Grange M, Sette C, Cuomo M, Conti M, Lagarde M, Prigent AF and Némaz G (2000) The cAMP-specific phosphodiesterase PDE4D3 is regulated by phosphatidic acid binding. Consequences for cAMP signaling pathway and characterization of a phosphatidic acid binding site. *J Biol Chem* **275**, 33379–33387.
 - 19 Frank R (2002) The SPOT-synthesis technique. Synthetic peptide arrays on membrane supports—principles and applications. *J Immunol Methods* **267**, 13–26.
 - 20 Cameron RT, Quinn SD, Cairns LS, MacLeod R, Samuel IDW, Smith BO, Carlos Penedo J and Baillie GS (2014) The phosphorylation of Hsp20 enhances its association with amyloid-beta to increase protection against neuronal cell death. *Mol Cell Neurosci* **61**, 46–55.
 - 21 Young RM (2019) Proximity ligation assay. *Methods Mol Biol* **1956**, 363–370.
 - 22 Bolger GB, McCahill A, Huston E, Cheung YF, McSorley T, Baillie GS and Houslay MD (2003) The unique amino-terminal region of the PDE4D5 cAMP phosphodiesterase isoform confers preferential interaction with beta-arrestins. *J Biol Chem* **278**, 49230–49238.
 - 23 Marchmont RJ and Houslay MD (1980) A peripheral and an intrinsic enzyme constitute the cyclic AMP phosphodiesterase activity of rat liver plasma membranes. *Biochem J* **187**, 381–392.
 - 24 Sin YY, Edwards HV, Li X, Day JP, Christian F, Dunlop AJ, Adams DR, Zaccolo M, Houslay MD and Baillie GS (2011) Disruption of the cyclic AMP phosphodiesterase-4 (PDE4)-HSP20 complex attenuates the beta-agonist induced hypertrophic response in cardiac myocytes. *J Mol Cell Cardiol* **50**, 872–883.
 - 25 Nikolaev VO, Bunemann M, Hein L, Hannawacker A and Loehse MJ (2004) Novel single chain cAMP sensors for receptor-induced signal propagation. *J Biol Chem* **279**, 37215–37218.
 - 26 Cong YF, Liu FW, Xu L, Song SS, Shen XR, Liu D, Hou XQ and Zhang HT (2023) Rolipram ameliorates memory deficits and depression-like behavior in APP/PS1/tau triple transgenic mice: involvement of neuroinflammation and apoptosis via cAMP signaling. *Int J Neuropsychopharmacol* **26**, 585–598.
 - 27 Wang H, Zhang FF, Xu Y, Fu HR, Wang XD, Wang L, Chen W, Xu XY, Gao YF, Zhang JG *et al.* (2020) The Phosphodiesterase-4 inhibitor roflumilast, a potential treatment for the comorbidity of memory loss and depression in Alzheimer's disease: a preclinical study in APP/PS1 transgenic mice. *Int J Neuropsychopharmacol* **23**, 700–711.
 - 28 Tibbo AJ, Mika D, Dobi S, Ling J, McFall A, Tejada GS, Blair C, MacLeod R, MacQuaide N, Gök C *et al.* (2022) Phosphodiesterase type 4 anchoring regulates cAMP signaling to Popeye domain-containing proteins. *J Mol Cell Cardiol* **165**, 86–102.
 - 29 Manczak M and Reddy PH (2012) Abnormal interaction of VDAC1 with amyloid beta and phosphorylated tau causes mitochondrial dysfunction in Alzheimer's disease. *Hum Mol Genet* **21**, 5131–5146.
 - 30 Brown KM, Day JP, Huston E, Zimmermann B, Hampel K, Christian F, Romano D, Terhzaz S, Lee LCY, Willis MJ *et al.* (2013) Phosphodiesterase-8A binds to and regulates Raf-1 kinase. *Proc Natl Acad Sci USA* **110**, E1533–E1542.
 - 31 Bolger GB, Baillie GS, Li X, Lynch MJ, Herzyk P, Mohamed A, High Mitchell L, McCahill A, Hundsrucker C, Klussmann E *et al.* (2006) Scanning peptide array analyses identify overlapping binding sites for the signalling scaffold proteins, beta-arrestin and RACK1, in cAMP-specific phosphodiesterase PDE4D5. *Biochem J* **398**, 23–36.
 - 32 Liu H, Wang Q, Huang Y, Deng J, Xie X, Zhu J, Yuan Y, He YM, Huang YY, Luo HB *et al.* (2022) Discovery of novel PDE4 inhibitors targeting the M-pocket from natural mangostanin with improved safety

- for the treatment of inflammatory bowel diseases. *Eur J Med Chem* **242**, 114631.
- 33 Nadezhdin KD, Bocharova OV, Bocharov EV and Arseniev AS (2012) Dimeric structure of transmembrane domain of amyloid precursor protein in micellar environment. *FEBS Lett* **586**, 1687–1692.
 - 34 Gurney ME, D'Amato EC and Burgin AB (2015) Phosphodiesterase-4 (PDE4) molecular pharmacology and Alzheimer's disease. *Neurotherapeutics* **12**, 49–56.
 - 35 Garcia-Osta A, Cuadrado-Tejedor M, Garcia-Barroso C, Oyarzabal J and Franco R (2012) Phosphodiesterases as therapeutic targets for Alzheimer's disease. *ACS Chem Neurosci* **3**, 832–844.
 - 36 Zhang C, Cheng Y, Wang H, Wang C, Wilson SP, Xu J and Zhang HT (2014) RNA interference-mediated knockdown of long-form phosphodiesterase-4D (PDE4D) enzyme reverses amyloid-beta42-induced memory deficits in mice. *J Alzheimers Dis* **38**, 269–280.
 - 37 Yu HY, Zhu Y, Zhang XL, Wang L, Zhou YM, Zhang FF, Zhang HT and Zhao XM (2022) Baicalin attenuates amyloid beta oligomers induced memory deficits and mitochondria fragmentation through regulation of PDE-PKA-Drp1 signalling. *Psychopharmacology (Berl)* **239**, 851–865.
 - 38 Olah J, Vincze O, Virók D, Simon D, Bozsó Z, Tökési N, Horváth I, Hlavanda E, Kovács J, Magyar A *et al.* (2011) Interactions of pathological hallmark proteins: tubulin polymerization promoting protein/p25, beta-amyloid, and alpha-synuclein. *J Biol Chem* **286**, 34088–34100.
 - 39 Gurney ME, Burgin AB, Magnusson OT and Stewart LJ (2011) Small molecule allosteric modulators of phosphodiesterase 4. *Handb Exp Pharmacol* 167–192.
 - 40 Omar F, Findlay JE, Carfray G, Allcock RW, Jiang Z, Moore C, Muir AL, Lannoy M, Fertig BA, Mai D *et al.* (2019) Small-molecule allosteric activators of PDE4 long form cyclic AMP phosphodiesterases. *Proc Natl Acad Sci USA* **116**, 13320–13329.
 - 41 Baillie GS, Tejada GS and Kelly MP (2019) Therapeutic targeting of 3',5'-cyclic nucleotide phosphodiesterases: inhibition and beyond. *Nat Rev Drug Discov* **18**, 770–796.
 - 42 Paes D, Schepers M, Rombaut B, van den Hove D, Vanmierlo T and Prickaerts J (2021) The molecular biology of phosphodiesterase 4 enzymes as pharmacological targets: an interplay of isoforms, conformational states, and inhibitors. *Pharmacol Rev* **73**, 1016–1049.
 - 43 Shuaib S, Saini RK, Goyal D and Goyal B (2020) Impact of K16A and K28A mutation on the structure and dynamics of amyloid-beta42 peptide in Alzheimer's disease: key insights from molecular dynamics simulations. *J Biomol Struct Dyn* **38**, 708–721.
 - 44 Tarus B, Straub JE and Thirumalai D (2006) Dynamics of Asp23-Lys28 salt-bridge formation in Aβ10-35 monomers. *J Am Chem Soc* **128**, 16159–16168.

Supporting information

Additional supporting information may be found online in the Supporting Information section at the end of the article.

Fig. S1. The PDE4D antibody does not cross-react with FAM-Aβ in a non-specific manner.

Fig. S2. The enzyme PDE4D and exogenously added Aβ co-localize in the cytoplasm of SH-SY5Y cells.

Fig. S3. PDE4D co-immunoprecipitates with exogenously added Aβ in SH-SY5Y cells.